

Measurement of the mass difference $m(B^0) - m(B^+)$

B. Aubert,¹ M. Bona,¹ Y. Karyotakis,¹ J. P. Lees,¹ V. Poireau,¹ E. Prencipe,¹ X. Prudent,¹ V. Tisserand,¹ J. Garra Tico,² E. Grauges,² L. Lopez,³ A. Palano,³ M. Pappagallo,³ G. Eigen,⁴ B. Stugu,⁴ L. Sun,⁴ G. S. Abrams,⁵ M. Battaglia,⁵ D. N. Brown,⁵ J. Button-Shafer,⁵ R. N. Cahn,⁵ R. G. Jacobsen,⁵ J. A. Kadyk,⁵ L. T. Kerth,⁵ Yu. G. Kolomensky,⁵ G. Kukartsev,⁵ G. Lynch,⁵ I. L. Osipenko,⁵ M. T. Ronan,^{5,*} K. Tackmann,⁵ T. Tanabe,⁵ W. A. Wenzel,⁵ C. M. Hawkes,⁶ N. Soni,⁶ A. T. Watson,⁶ H. Koch,⁷ T. Schroeder,⁷ D. Walker,⁸ D. J. Asgeirsson,⁹ T. Cuhadar-Donszelmann,⁹ B. G. Fulsom,⁹ C. Hearty,⁹ T. S. Mattison,⁹ J. A. McKenna,⁹ M. Barrett,¹⁰ A. Khan,¹⁰ M. Saleem,¹⁰ L. Teodorescu,¹⁰ V. E. Blinov,¹¹ A. D. Bukin,¹¹ A. R. Buzykaev,¹¹ V. P. Druzhinin,¹¹ V. B. Golubev,¹¹ A. P. Onuchin,¹¹ S. I. Serednyakov,¹¹ Yu. I. Skovpen,¹¹ E. P. Solodov,¹¹ K. Yu. Todyshev,¹¹ M. Bondioli,¹² S. Curry,¹² I. Eschrich,¹² D. Kirkby,¹² A. J. Lankford,¹² P. Lund,¹² M. Mandelkern,¹² E. C. Martin,¹² D. P. Stoker,¹² S. Abachi,¹³ C. Buchanan,¹³ J. W. Gary,¹⁴ F. Liu,¹⁴ O. Long,¹⁴ B. C. Shen,^{14,*} G. M. Vitug,¹⁴ Z. Yasin,¹⁴ L. Zhang,¹⁴ V. Sharma,¹⁵ C. Campagnari,¹⁶ T. M. Hong,¹⁶ D. Kovalskyi,¹⁶ M. A. Mazur,¹⁶ J. D. Richman,¹⁶ T. W. Beck,¹⁷ A. M. Eisner,¹⁷ C. J. Flacco,¹⁷ C. A. Heusch,¹⁷ J. Kroseberg,¹⁷ W. S. Lockman,¹⁷ T. Schalk,¹⁷ B. A. Schumm,¹⁷ A. Seiden,¹⁷ L. Wang,¹⁷ M. G. Wilson,¹⁷ L. O. Winstrom,¹⁷ C. H. Cheng,¹⁸ D. A. Doll,¹⁸ B. Echenard,¹⁸ F. Fang,¹⁸ D. G. Hitlin,¹⁸ I. Narsky,¹⁸ T. Piatenko,¹⁸ F. C. Porter,¹⁸ R. Andreassen,¹⁹ G. Mancinelli,¹⁹ B. T. Meadows,¹⁹ K. Mishra,¹⁹ M. D. Sokoloff,¹⁹ F. Blanc,²⁰ P. C. Bloom,²⁰ W. T. Ford,²⁰ A. Gaz,²⁰ J. F. Hirschauer,²⁰ A. Kreisel,²⁰ M. Nagel,²⁰ U. Nauenberg,²⁰ A. Olivas,²⁰ J. G. Smith,²⁰ K. A. Ulmer,²⁰ S. R. Wagner,²⁰ R. Ayad,^{21,+} A. M. Gabareen,²¹ A. Soffer,^{21,*} W. H. Toki,²¹ R. J. Wilson,²¹ D. D. Altenburg,²² E. Feltresi,²² A. Hauke,²² H. Jasper,²² M. Karbach,²² J. Merkel,²² A. Petzold,²² B. Spaan,²² K. Wacker,²² V. Klose,²³ M. J. Kobel,²³ H. M. Lacker,²³ W. F. Mader,²³ R. Nogowski,²³ K. R. Schubert,²³ R. Schwierz,²³ J. E. Sundermann,²³ A. Volk,²³ D. Bernard,²⁴ G. R. Bonneaud,²⁴ E. Latour,²⁴ Ch. Thiebaut,²⁴ M. Verderi,²⁴ P. J. Clark,²⁵ W. Gradl,²⁵ S. Playfer,²⁵ J. E. Watson,²⁵ M. Andreotti,²⁶ D. Bettoni,²⁶ C. Bozzi,²⁶ R. Calabrese,²⁶ A. Cecchi,²⁶ G. Cibinetto,²⁶ P. Franchini,²⁶ E. Luppi,²⁶ M. Negrini,²⁶ A. Petrella,²⁶ L. Piemontese,²⁶ V. Santoro,²⁶ F. Anulli,²⁷ R. Baldini-Ferroli,²⁷ A. Calcaterra,²⁷ R. de Sangro,²⁷ G. Finocchiaro,²⁷ S. Pacetti,²⁷ P. Patteri,²⁷ I. M. Peruzzi,^{27,§} M. Piccolo,²⁷ M. Rama,²⁷ A. Zallo,²⁷ A. Buzzo,²⁸ R. Contri,²⁸ M. Lo Vetere,²⁸ M. M. Macri,²⁸ M. R. Monge,²⁸ S. Passaggio,²⁸ C. Patrignani,²⁸ E. Robutti,²⁸ A. Santroni,²⁸ S. Tosi,²⁸ K. S. Chaisanguanthum,²⁹ M. Morii,²⁹ R. S. Dubitzky,³⁰ J. Marks,³⁰ S. Schenk,³⁰ U. Uwer,³⁰ D. J. Bard,³¹ P. D. Dauncey,³¹ J. A. Nash,³¹ W. Panduro Vazquez,³¹ M. Tibbetts,³¹ P. K. Behera,³² X. Chai,³² M. J. Charles,³² U. Mallik,³² J. Cochran,³³ H. B. Crawley,³³ L. Dong,³³ W. T. Meyer,³³ S. Prell,³³ E. I. Rosenberg,³³ A. E. Rubin,³³ Y. Y. Gao,³⁴ A. V. Gritsan,³⁴ Z. J. Guo,³⁴ C. K. Lae,³⁴ A. G. Denig,³⁵ M. Fritsch,³⁵ G. Schott,³⁵ N. Arnaud,³⁶ J. Béquilleux,³⁶ A. D'Orazio,³⁶ M. Davier,³⁶ J. Firmino da Costa,³⁶ G. Grosdidier,³⁶ A. Höcker,³⁶ V. Lepeltier,³⁶ F. Le Diberder,³⁶ A. M. Lutz,³⁶ S. Pruvot,³⁶ P. Roudeau,³⁶ M. H. Schune,³⁶ J. Serrano,³⁶ V. Sordini,³⁶ A. Stocchi,³⁶ W. F. Wang,³⁶ G. Wormser,³⁶ D. J. Lange,³⁷ D. M. Wright,³⁷ I. Bingham,³⁸ J. P. Burke,³⁸ C. A. Chavez,³⁸ J. R. Fry,³⁸ E. Gabathuler,³⁸ R. Gamet,³⁸ D. E. Hutchcroft,³⁸ D. J. Payne,³⁸ C. Touramanis,³⁸ A. J. Bevan,³⁹ K. A. George,³⁹ F. Di Lodovico,³⁹ R. Sacco,³⁹ M. Sigamani,³⁹ G. Cowan,⁴⁰ H. U. Flaecher,⁴⁰ D. A. Hopkins,⁴⁰ S. Paramesvaran,⁴⁰ F. Salvatore,⁴⁰ A. C. Wren,⁴⁰ D. N. Brown,⁴¹ C. L. Davis,⁴¹ K. E. Alwyn,⁴² N. R. Barlow,⁴² R. J. Barlow,⁴² Y. M. Chia,⁴² C. L. Edgar,⁴² G. D. Lafferty,⁴² T. J. West,⁴² J. I. Yi,⁴² J. Anderson,⁴³ C. Chen,⁴³ A. Jawahery,⁴³ D. A. Roberts,⁴³ G. Simi,⁴³ J. M. Tuggle,⁴³ C. Dallapiccola,⁴⁴ S. S. Hertzbach,⁴⁴ X. Li,⁴⁴ E. Salvati,⁴⁴ S. Saremi,⁴⁴ R. Cowan,⁴⁵ D. Dujmic,⁴⁵ P. H. Fisher,⁴⁵ K. Koenke,⁴⁵ G. Sciolla,⁴⁵ M. Spitznagel,⁴⁵ F. Taylor,⁴⁵ R. K. Yamamoto,⁴⁵ M. Zhao,⁴⁵ S. E. Mclachlin,^{46,*} P. M. Patel,⁴⁶ S. H. Robertson,⁴⁶ A. Lazzaro,⁴⁷ V. Lombardo,⁴⁷ F. Palombo,⁴⁷ J. M. Bauer,⁴⁸ L. Cremaldi,⁴⁸ V. Eschenburg,⁴⁸ R. Godang,⁴⁸ R. Kroeger,⁴⁸ D. A. Sanders,⁴⁸ D. J. Summers,⁴⁸ H. W. Zhao,⁴⁸ S. Brunet,⁴⁹ D. Côté,⁴⁹ M. Simard,⁴⁹ P. Taras,⁴⁹ F. B. Viaud,⁴⁹ H. Nicholson,⁵⁰ G. De Nardo,⁵¹ L. Lista,⁵¹ D. Monorchio,⁵¹ C. Sciacca,⁵¹ M. A. Baak,⁵² G. Raven,⁵² H. L. Snoek,⁵² C. P. Jessop,⁵³ K. J. Knoepfel,⁵³ J. M. LoSecco,⁵³ G. Benelli,⁵⁴ L. A. Corwin,⁵⁴ K. Honscheid,⁵⁴ H. Kagan,⁵⁴ R. Kass,⁵⁴ J. P. Morris,⁵⁴ A. M. Rahimi,⁵⁴ J. J. Regensburger,⁵⁴ S. J. Sekula,⁵⁴ Q. K. Wong,⁵⁴ N. L. Blount,⁵⁵ J. Brau,⁵⁵ R. Frey,⁵⁵ O. Igonkina,⁵⁵ J. A. Kolb,⁵⁵ M. Lu,⁵⁵ R. Rahmat,⁵⁵ N. B. Sinev,⁵⁵ D. Strom,⁵⁵ J. Strube,⁵⁵ E. Torrence,⁵⁵ G. Castelli,⁵⁶ N. Gagliardi,⁵⁶ M. Margoni,⁵⁶ M. Morandin,⁵⁶ M. Posocco,⁵⁶ M. Rotondo,⁵⁶ F. Simonetto,⁵⁶ R. Stroili,⁵⁶ C. Voci,⁵⁶ P. del Amo Sanchez,⁵⁷ E. Ben-Haim,⁵⁷ H. Briand,⁵⁷ G. Calderini,⁵⁷ J. Chauveau,⁵⁷ P. David,⁵⁷ L. Del Buono,⁵⁷ O. Hamon,⁵⁷ Ph. Leruste,⁵⁷ J. Ocariz,⁵⁷ A. Perez,⁵⁷ J. Prendki,⁵⁷ L. Gladney,⁵⁸ M. Biasini,⁵⁹ R. Covarelli,⁵⁹ E. Manoni,⁵⁹ C. Angelini,⁶⁰ G. Batignani,⁶⁰ S. Bettarini,⁶⁰ M. Carpinelli,^{60,||} A. Cervelli,⁶⁰ F. Forti,⁶⁰ M. A. Giorgi,⁶⁰ A. Lusiani,⁶⁰ G. Marchiori,⁶⁰ M. Morganti,⁶⁰ N. Neri,⁶⁰ E. Paoloni,⁶⁰ G. Rizzo,⁶⁰ J. J. Walsh,⁶⁰ J. Biesiada,⁶¹ D. Lopes Pegna,⁶¹ C. Lu,⁶¹ J. Olsen,⁶¹ A. J. S. Smith,⁶¹ A. V. Telnov,⁶¹ E. Baracchini,⁶² G. Cavoto,⁶² D. del Re,⁶² E. Di Marco,⁶² R. Faccini,⁶² F. Ferrarotto,⁶²

F. Ferroni,⁶² M. Gaspero,⁶² P. D. Jackson,⁶² L. Li Gioi,⁶² M. A. Mazzoni,⁶² S. Morganti,⁶² G. Piredda,⁶² F. Polci,⁶² F. Renga,⁶² C. Voena,⁶² M. Ebert,⁶³ T. Hartmann,⁶³ H. Schröder,⁶³ R. Waldi,⁶³ T. Adye,⁶⁴ B. Franek,⁶⁴ E. O. Olaiya,⁶⁴ W. Roethel,⁶⁴ F. F. Wilson,⁶⁴ S. Emery,⁶⁵ M. Escalier,⁶⁵ L. Esteve,⁶⁵ A. Gaidot,⁶⁵ S. F. Ganzhur,⁶⁵ G. Hamel de Monchenault,⁶⁵ W. Kozanecki,⁶⁵ G. Vasseur,⁶⁵ Ch. Yèche,⁶⁵ M. Zito,⁶⁵ X. R. Chen,⁶⁶ H. Liu,⁶⁶ W. Park,⁶⁶ M. V. Purohit,⁶⁶ R. M. White,⁶⁶ J. R. Wilson,⁶⁶ M. T. Allen,⁶⁷ D. Aston,⁶⁷ R. Bartoldus,⁶⁷ P. Bechtel,⁶⁷ J. F. Benitez,⁶⁷ R. Cenci,⁶⁷ J. P. Coleman,⁶⁷ M. R. Convery,⁶⁷ J. C. Dingfelder,⁶⁷ J. Dorfan,⁶⁷ G. P. Dubois-Felsmann,⁶⁷ W. Dunwoodie,⁶⁷ R. C. Field,⁶⁷ S. J. Gowdy,⁶⁷ M. T. Graham,⁶⁷ P. Grenier,⁶⁷ C. Hast,⁶⁷ W. R. Innes,⁶⁷ J. Kaminski,⁶⁷ M. H. Kelsey,⁶⁷ H. Kim,⁶⁷ P. Kim,⁶⁷ M. L. Kocian,⁶⁷ D. W. G. S. Leith,⁶⁷ S. Li,⁶⁷ B. Lindquist,⁶⁷ S. Luitz,⁶⁷ V. Luth,⁶⁷ H. L. Lynch,⁶⁷ D. B. MacFarlane,⁶⁷ H. Marsiske,⁶⁷ R. Messner,⁶⁷ D. R. Muller,⁶⁷ H. Neal,⁶⁷ S. Nelson,⁶⁷ C. P. O'Grady,⁶⁷ I. Ofte,⁶⁷ A. Perazzo,⁶⁷ M. Perl,⁶⁷ B. N. Ratcliff,⁶⁷ A. Roodman,⁶⁷ A. A. Salnikov,⁶⁷ R. H. Schindler,⁶⁷ J. Schwiening,⁶⁷ A. Snyder,⁶⁷ D. Su,⁶⁷ M. K. Sullivan,⁶⁷ K. Suzuki,⁶⁷ S. K. Swain,⁶⁷ J. M. Thompson,⁶⁷ J. Va'vra,⁶⁷ A. P. Wagner,⁶⁷ M. Weaver,⁶⁷ C. A. West,⁶⁷ W. J. Wisniewski,⁶⁷ M. Wittgen,⁶⁷ D. H. Wright,⁶⁷ H. W. Wulsin,⁶⁷ A. K. Yarritu,⁶⁷ K. Yi,⁶⁷ C. C. Young,⁶⁷ V. Ziegler,⁶⁷ P. R. Burchat,⁶⁸ A. J. Edwards,⁶⁸ S. A. Majewski,⁶⁸ T. S. Miyashita,⁶⁸ B. A. Petersen,⁶⁸ L. Wilden,⁶⁸ S. Ahmed,⁶⁹ M. S. Alam,⁶⁹ R. Bula,⁶⁹ J. A. Ernst,⁶⁹ B. Pan,⁶⁹ M. A. Saeed,⁶⁹ S. B. Zain,⁶⁹ S. M. Spanier,⁷⁰ B. J. Wogslund,⁷⁰ R. Eckmann,⁷¹ J. L. Ritchie,⁷¹ A. M. Ruland,⁷¹ C. J. Schilling,⁷¹ R. F. Schwitters,⁷¹ B. W. Drummond,⁷² J. M. Izen,⁷² X. C. Lou,⁷² S. Ye,⁷² F. Bianchi,⁷³ D. Gamba,⁷³ M. Pelliccioni,⁷³ M. Bomben,⁷⁴ L. Bosisio,⁷⁴ C. Cartaro,⁷⁴ G. Della Ricca,⁷⁴ L. Lanceri,⁷⁴ L. Vitale,⁷⁴ V. Azzolini,⁷⁵ N. Lopez-March,⁷⁵ F. Martinez-Vidal,⁷⁵ D. A. Milanes,⁷⁵ A. Oyanguren,⁷⁵ J. Albert,⁷⁶ Sw. Banerjee,⁷⁶ B. Bhuyan,⁷⁶ H. H. F. Choi,⁷⁶ K. Hamano,⁷⁶ R. Kowalewski,⁷⁶ M. J. Lewczuk,⁷⁶ I. M. Nugent,⁷⁶ J. M. Roney,⁷⁶ R. J. Sobie,⁷⁶ T. J. Gershon,⁷⁷ P. F. Harrison,⁷⁷ J. Ilc,⁷⁷ T. E. Latham,⁷⁷ G. B. Mohanty,⁷⁷ H. R. Band,⁷⁸ X. Chen,⁷⁸ S. Dasu,⁷⁸ K. T. Flood,⁷⁸ Y. Pan,⁷⁸ M. Pierini,⁷⁸ R. Prepost,⁷⁸ C. O. Vuosalo,⁷⁸ and S. L. Wu⁷⁸

(BABAR Collaboration)

¹Laboratoire de Physique des Particules, IN2P3/CNRS et Université de Savoie, F-74941 Annecy-Le-Vieux, France

²Universitat de Barcelona, Facultat de Física, Departament ECM, E-08028 Barcelona, Spain

³Università di Bari, Dipartimento di Fisica and INFN, I-70126 Bari, Italy

⁴University of Bergen, Institute of Physics, N-5007 Bergen, Norway

⁵Lawrence Berkeley National Laboratory and University of California, Berkeley, California 94720, USA

⁶University of Birmingham, Birmingham, B15 2TT, United Kingdom

⁷Ruhr Universität Bochum, Institut für Experimentalphysik I, D-44780 Bochum, Germany

⁸University of Bristol, Bristol BS8 1TL, United Kingdom

⁹University of British Columbia, Vancouver, British Columbia, Canada V6T 1Z1

¹⁰Brunel University, Uxbridge, Middlesex UB8 3PH, United Kingdom

¹¹Budker Institute of Nuclear Physics, Novosibirsk 630090, Russia

¹²University of California at Irvine, Irvine, California 92697, USA

¹³University of California at Los Angeles, Los Angeles, California 90024, USA

¹⁴University of California at Riverside, Riverside, California 92521, USA

¹⁵University of California at San Diego, La Jolla, California 92093, USA

¹⁶University of California at Santa Barbara, Santa Barbara, California 93106, USA

¹⁷University of California at Santa Cruz, Institute for Particle Physics, Santa Cruz, California 95064, USA

¹⁸California Institute of Technology, Pasadena, California 91125, USA

¹⁹University of Cincinnati, Cincinnati, Ohio 45221, USA

²⁰University of Colorado, Boulder, Colorado 80309, USA

²¹Colorado State University, Fort Collins, Colorado 80523, USA

²²Technische Universität Dortmund, Fakultät Physik, D-44221 Dortmund, Germany

²³Technische Universität Dresden, Institut für Kern- und Teilchenphysik, D-01062 Dresden, Germany

²⁴Laboratoire Leprince-Ringuet, CNRS/IN2P3, Ecole Polytechnique, F-91128 Palaiseau, France

²⁵University of Edinburgh, Edinburgh EH9 3JZ, United Kingdom

²⁶Università di Ferrara, Dipartimento di Fisica and INFN, I-44100 Ferrara, Italy

²⁷Laboratori Nazionali di Frascati dell'INFN, I-00044 Frascati, Italy

²⁸Università di Genova, Dipartimento di Fisica and INFN, I-16146 Genova, Italy

²⁹Harvard University, Cambridge, Massachusetts 02138, USA

³⁰Universität Heidelberg, Physikalisches Institut, Philosophenweg 12, D-69120 Heidelberg, Germany

³¹Imperial College London, London, SW7 2AZ, United Kingdom

³²University of Iowa, Iowa City, Iowa 52242, USA

³³Iowa State University, Ames, Iowa 50011-3160, USA

- ³⁴*Johns Hopkins University, Baltimore, Maryland 21218, USA*
- ³⁵*Universität Karlsruhe, Institut für Experimentelle Kernphysik, D-76021 Karlsruhe, Germany*
- ³⁶*Laboratoire de l'Accélérateur Linéaire, IN2P3/CNRS et Université Paris-Sud 11, Centre Scientifique d'Orsay, B. P. 34, F-91898 ORSAY Cedex, France*
- ³⁷*Lawrence Livermore National Laboratory, Livermore, California 94550, USA*
- ³⁸*University of Liverpool, Liverpool L69 7ZE, United Kingdom*
- ³⁹*Queen Mary, University of London, E1 4NS, United Kingdom*
- ⁴⁰*University of London, Royal Holloway and Bedford New College, Egham, Surrey TW20 0EX, United Kingdom*
- ⁴¹*University of Louisville, Louisville, Kentucky 40292, USA*
- ⁴²*University of Manchester, Manchester M13 9PL, United Kingdom*
- ⁴³*University of Maryland, College Park, Maryland 20742, USA*
- ⁴⁴*University of Massachusetts, Amherst, Massachusetts 01003, USA*
- ⁴⁵*Massachusetts Institute of Technology, Laboratory for Nuclear Science, Cambridge, Massachusetts 02139, USA*
- ⁴⁶*McGill University, Montréal, Québec, Canada H3A 2T8*
- ⁴⁷*Università di Milano, Dipartimento di Fisica and INFN, I-20133 Milano, Italy*
- ⁴⁸*University of Mississippi, University, Mississippi 38677, USA*
- ⁴⁹*Université de Montréal, Physique des Particules, Montréal, Québec, Canada H3C 3J7*
- ⁵⁰*Mount Holyoke College, South Hadley, Massachusetts 01075, USA*
- ⁵¹*Università di Napoli Federico II, Dipartimento di Scienze Fisiche and INFN, I-80126, Napoli, Italy*
- ⁵²*NIKHEF, National Institute for Nuclear Physics and High Energy Physics, NL-1009 DB Amsterdam, The Netherlands*
- ⁵³*University of Notre Dame, Notre Dame, Indiana 46556, USA*
- ⁵⁴*Ohio State University, Columbus, Ohio 43210, USA*
- ⁵⁵*University of Oregon, Eugene, Oregon 97403, USA*
- ⁵⁶*Università di Padova, Dipartimento di Fisica and INFN, I-35131 Padova, Italy*
- ⁵⁷*Laboratoire de Physique Nucléaire et de Hautes Energies, IN2P3/CNRS, Université Pierre et Marie Curie-Paris6, Université Denis Diderot-Paris7, F-75252 Paris, France*
- ⁵⁸*University of Pennsylvania, Philadelphia, Pennsylvania 19104, USA*
- ⁵⁹*Università di Perugia, Dipartimento di Fisica and INFN, I-06100 Perugia, Italy*
- ⁶⁰*Università di Pisa, Dipartimento di Fisica, Scuola Normale Superiore and INFN, I-56127 Pisa, Italy*
- ⁶¹*Princeton University, Princeton, New Jersey 08544, USA*
- ⁶²*Università di Roma La Sapienza, Dipartimento di Fisica and INFN, I-00185 Roma, Italy*
- ⁶³*Universität Rostock, D-18051 Rostock, Germany*
- ⁶⁴*Rutherford Appleton Laboratory, Chilton, Didcot, Oxon, OX11 0QX, United Kingdom*
- ⁶⁵*DSM/Dapnia, CEA/Saclay, F-91191 Gif-sur-Yvette, France*
- ⁶⁶*University of South Carolina, Columbia, South Carolina 29208, USA*
- ⁶⁷*Stanford Linear Accelerator Center, Stanford, California 94309, USA*
- ⁶⁸*Stanford University, Stanford, California 94305-4060, USA*
- ⁶⁹*State University of New York, Albany, New York 12222, USA*
- ⁷⁰*University of Tennessee, Knoxville, Tennessee 37996, USA*
- ⁷¹*University of Texas at Austin, Austin, Texas 78712, USA*
- ⁷²*University of Texas at Dallas, Richardson, Texas 75083, USA*
- ⁷³*Università di Torino, Dipartimento di Fisica Sperimentale and INFN, I-10125 Torino, Italy*
- ⁷⁴*Università di Trieste, Dipartimento di Fisica and INFN, I-34127 Trieste, Italy*
- ⁷⁵*IFIC, Universitat de Valencia-CSIC, E-46071 Valencia, Spain*
- ⁷⁶*University of Victoria, Victoria, British Columbia, Canada V8W 3P6*
- ⁷⁷*Department of Physics, University of Warwick, Coventry CV4 7AL, United Kingdom*
- ⁷⁸*University of Wisconsin, Madison, Wisconsin 53706, USA*

(Received 6 May 2008; published 15 July 2008)

Using 230×10^6 $B\bar{B}$ events recorded with the BABAR detector at the e^+e^- storage rings PEP-II, we reconstruct approximately 4100 $B^0 \rightarrow J/\psi K^+ \pi^-$ and 9930 $B^+ \rightarrow J/\psi K^+$ decays with $J/\psi \rightarrow \mu^+ \mu^-$ and $e^+ e^-$. From the measured B -momentum distributions in the e^+e^- rest frame, we determine the mass difference $m(B^0) - m(B^+) = (+0.33 \pm 0.05 \pm 0.03) \text{ MeV}/c^2$.

DOI: [10.1103/PhysRevD.78.011103](https://doi.org/10.1103/PhysRevD.78.011103)

PACS numbers: 13.25.Hw, 13.40.Dk, 14.40.Nd

*Deceased

[†]Now at Temple University, Philadelphia, PA 19122, USA.

^{*}Now at Tel Aviv University, Tel Aviv, 69978, Israel.

[§]Also with Università di Perugia, Dipartimento di Fisica, Perugia, Italy.

^{||}Also with Università di Sassari, Sassari, Italy.

Mass differences $\Delta m_M = m(M^0) - m(M^+)$ probe the size of Coulomb contributions to the quark structure of pseudoscalar mesons M . The values of Δm_M for π , K , and D mesons are experimentally well known; in units of MeV/c^2 they are $\Delta m_\pi = -4.5936 \pm 0.0005$, $\Delta m_K = +3.97 \pm 0.03$, and $\Delta m_D = -4.78 \pm 0.10$ [1]. For B mesons, $\Delta m_B = (+0.37 \pm 0.24) \text{ MeV}/c^2$ [2] is less precise and compatible with zero. Quark-model calculations [3] give Δm_B near $+0.3 \text{ MeV}/c^2$ but are quite uncertain since the contributions from the quark-mass difference $m(d) - m(u)$ and from the Coulomb effects have similar magnitudes and opposite signs. In the case of Δm_D , the two contributions enter with the same signs.

The value of Δm_B is an important input for estimating the decay ratio $R = \Gamma[Y(4S) \rightarrow B^+ B^-] / \Gamma[Y(4S) \rightarrow B^0 \bar{B}^0]$ which in turn is essential for determining B^+ and B^0 decay fractions at e^+e^- colliders where B mesons are produced in decays of the $Y(4S)$. The leading contribution to R is given by the vector nature of the matrix element and by kinematics; at fixed energy it is

$$R_0 = [p^*(B^+)/p^*(B^0)]^3 \approx 1 + 3m_B \Delta m_B / p_B^{*2}, \quad (1)$$

where $p^*(B^+)$ and $p^*(B^0)$ are the B^+ and B^0 momenta in the center-of-mass system (cms) at this energy, and p_B^* and m_B are the mean values of the two momenta and masses, respectively. For $|\Delta m_B|$ below $0.5 \text{ MeV}/c^2$, the quark structures of $Y(4S)$ and B mesons and the Coulomb interaction [4] may lead to $|R - R_0| > R_0 - 1$.

For measuring Δm_B , we use 210 fb^{-1} of e^+e^- annihilation data recorded on the $Y(4S)$ resonance with the BABAR detector [5] at the SLAC e^+e^- storage rings PEP-II [6]. Charged-particle momenta are measured by the tracking system consisting of a five-layer double-sided silicon vertex tracker and a 40-layer drift chamber, both located in a 1.5 T magnetic field of a superconducting solenoid. Transverse momenta p_T are determined with a resolution of about $\sigma(p_T)/p_T = 0.0013 \times p_T/\text{GeV} + 0.0045$ and track angles with resolutions around 0.4 mrad .

The B mesons are reconstructed in two decay modes with low background level: $B^0 \rightarrow J/\psi K^+ \pi^-$ and $B^+ \rightarrow J/\psi K^+$ [7], where $J/\psi \rightarrow \mu^+ \mu^-$ or $e^+ e^-$ in both modes. Measurements of K^0 and J/ψ invariant masses show that relative momentum uncertainties $\delta p/p$, originating from the limited knowledge of the magnetic field and the charged-particle energy losses, are below 4×10^{-4} . A momentum uncertainty of this size leads to B -meson mass uncertainties of the order of $1 \text{ MeV}/c^2$. The mass difference Δm_B can be determined with much higher precision using B -meson momenta because the decay $Y(4S) \rightarrow B \bar{B}$ produces B mesons with low momenta, $p^*(B) \approx 320 \text{ MeV}/c$. At fixed cms energy \sqrt{s} we have

$$m^2(B^+)c^2 + p^{*2}(B^+) = m^2(B^0)c^2 + p^{*2}(B^0), \quad (2)$$

$$\Delta m_B = -\Delta p^* \times \frac{p^*(B^0) + p^*(B^+)}{[m(B^0) + m(B^+)]c^2} \quad (3)$$

where $\Delta p^* = p^*(B^0) - p^*(B^+)$. The track-momentum uncertainties lead to $\delta p^* < 4 \times 10^{-4} \times 320 \text{ MeV}/c$, $\delta(\Delta p^*) \leq \sqrt{2} \times \delta p^*$, and, using Eq. (3), $\delta(\Delta m_B) < 0.01 \text{ MeV}/c^2$ which is 2 orders of magnitude smaller than the $1 \text{ MeV}/c^2$ estimate using invariant masses.

The energy spread of the PEP-II beams gives a \sqrt{s} distribution with a rms width of about 5 MeV , resulting in broad distributions of the true momenta $p_{\text{true}}^*(B)$ with rms widths of about $40 \text{ MeV}/c$. The reconstructed p^* spectra are only slightly wider since the detector resolution is only $\sigma(p^* - p_{\text{true}}^*) \approx 15 \text{ MeV}/c$ in the selected B -decay modes, where σ is the rms width. As input for Eq. (3), we use the mean values $\hat{p}^*(B^0)$ and $\hat{p}^*(B^+)$ of the reconstructed p^* spectra. The presence of background prevents the two \hat{p}^* values from being obtained as algebraic means of all measured p^* values. Instead, they are determined from fits with analytic functions for the signal and the background shapes.

The size of a possible bias from the mean- p^* method is estimated by Monte Carlo (MC) simulations in two steps. The influence of the beam smearing and the $Y(4S)$ line shape is studied by determining the means $\hat{p}_{\text{true}}^*(B)$ using a MC simulation in the cms without detector. We use a Gaussian cms-energy distribution with two parameters: \sqrt{s}_{mean} and $\sigma_{\sqrt{s}}$, and $Y(4S) \rightarrow B \bar{B}$ line shapes with four parameters: $m(Y(4S))$, $m(B^0)$, $m(B^+)$, and Γ_0 , where the latter is the total width at $s = m^2(Y(4S))$. The line shape is parametrized following Ref. [8]; it includes initial state radiation, a relativistic Breit-Wigner function with energy-dependent width, $m(B)$ - and s -dependent phase space factors, and meson-structure effects. Because of the $m(B)$ dependence of the phase space factor, the line shapes differ for B^0 and B^+ . We fix Δm_B to either $+0.3$ or $+0.4 \text{ MeV}/c^2$ and vary the other parameters in the range of the results of Ref. [8]. We determine $\hat{p}_{\text{true}}^*(B^0)$ and $\hat{p}_{\text{true}}^*(B^+)$ for each set of parameters and find that the derived Δm_B results from Eq. (3) are equal to the MC input within $\pm 2\%$. The rms widths σ_{p^*} of the two p_{true}^* distributions are found to be different in agreement with

$$\sigma_{p^*}(B^+)/\sigma_{p^*}(B^0) = \hat{p}^*(B^0)/\hat{p}^*(B^+), \quad (4)$$

as simple consequence of Eq. (2).

The detector influence on the Δm_B bias is studied by a full MC simulation of generic $B \bar{B}$ decays with GEANT4 [9]. The simulation includes all detector and reconstruction effects and the same Gaussian cms-energy distribution as above, but uses a simpler $Y(4S) \rightarrow B \bar{B}$ line shape with fixed $\Gamma(s)$, without initial state radiation, and without meson-structure effects. The results on the means of $p^* - p_{\text{true}}^*$ are given in the discussion of the systematic uncertainties.

The same GEANT4-based MC simulation is used to determine the selection criteria for B reconstruction and to find the fit-function types for signal and background in the reconstructed p^* spectra. The J/ψ decays into $\mu\mu$ and ee are studied separately in order to control the influences of bremsstrahlung in the ee channel, simulated by PHOTOS [10] and GEANT4. Muons are identified using a neural network with a high efficiency of 0.90 accepting a rather high probability for pion misidentification (misid) of 0.08, while electrons are identified using a likelihood selector with an efficiency of 0.95 and a pion-misid probability of 10^{-3} . Electron tracks are combined with up to three nearby photons into electron candidates using a bremsstrahlung-recovery algorithm. Pairs of electrons or muons with opposite charge are fitted to a common vertex. All pairs with a vertex fit probability $P > 10^{-4}$ and an invariant mass between 3.057 and 3.137 GeV/c^2 are selected as J/ψ candidates. Because of background from two pions in jetlike $e^+e^- \rightarrow q\bar{q}$ events, we also require $|\cos(\theta_H)| < 0.9$ for $J/\psi \rightarrow \mu\mu$ candidates, where θ_H is the angle between one muon and the B candidate in the J/ψ rest frame. Since the pion misid is much lower for electrons, this cut is not applied in the $J/\psi \rightarrow ee$ mode. In the B^0 mode with $J/\psi \rightarrow \mu\mu$ we require in addition that the normalized second Fox-Wolfram moment R_2 [11] of the event is less than 0.4.

Charged kaons are identified using a likelihood selector, based on the DIRC system [12] of BABAR, with an efficiency of 0.95 and a pion-misid probability of 0.05. The $K\pi$ pairs are formed from two oppositely charged tracks, one identified as a kaon and the other as a pion; the fit to a common vertex must give a fit probability $P > 10^{-4}$. For suppressing background, we require an invariant mass $m(K\pi) = m(K^{*0}) \pm 75 \text{ MeV}/c^2$. The B^0 and B^+ candidates are formed by combining the J/ψ with the $K\pi$ -pair candidates and with charged tracks identified as kaons, respectively. We also require a fit probability $P > 10^{-4}$ for the common vertex. The B candidates are further selected by their value of $\Delta E^* = E_B^* - \sqrt{s}/2$, where E_B^* is the energy of the B candidate in the cms.

To optimize signal versus background in the p^* distributions and to account for bremsstrahlung, we have chosen four different ΔE^* selection criteria. For $J/\psi \rightarrow \mu\mu$ we choose $|\Delta E^*| < 55 \text{ MeV}$ for the B^+ and $|\Delta E^*| < 25 \text{ MeV}$ for the B^0 . For $J/\psi \rightarrow ee$ we take $-60 < \Delta E^* < 50 \text{ MeV}$ and $-30 < \Delta E^* < 20 \text{ MeV}$ in B^+ and B^0 decays, respectively. For the B^+ this corresponds to ± 3 rms widths of the signal, for the B^0 to ± 1.5 rms. The tighter criteria in B^0 decays, where the background is an important contribution to the final systematic uncertainty on Δm_B , are justified by the negligible correlations between ΔE^* and p^* and by the MC validation as described below. After applying the ΔE^* criteria to the B candidates, there remain events with more than one candidate. The fraction is negligible for B^+ (0.10% of all events) but is 1.5% for B^0 . If there are

multiple B candidates in the event, we choose the one with the best B -vertex fit. The selection criteria for data and MC events are identical with one exception: In the data, because of a bias in the J/ψ mass reconstruction owing to track-momentum uncertainties, the lower and upper limits for $m(\mu\mu)$ and $m(ee)$ are shifted by $-2 \text{ MeV}/c^2$.

Figure 1 shows the p^* distributions of the selected data and those from the MC simulation. The MC distributions are normalized to the data between 0.12 and 0.45 GeV/c . They contain contributions from four classes,

Class 1, “pure signal,” candidates where all tracks originate from true B -decay particles into the given mode and where the decays contain no photons including those combined into electron candidates with the bremsstrahlung-recovery algorithm,

Class 2, “signal with radiation,” like pure signal, but with at least one photon from bremsstrahlung generated by PHOTOS or GEANT4,

Class 3, “ $B\bar{B}$ background,” candidates from B decays other than from classes 1 or 2 and

Class 4, “ $q\bar{q}$ background,” candidates from non- $B\bar{B}$ events.

The third class also contains some signal events with wrong matching of reconstructed and generated tracks. As can clearly be seen, the $B\bar{B}$ background in B^0 decays is larger than in B^+ decays and the fraction of candidates with bremsstrahlung is larger in the $J/\psi \rightarrow ee$ than in the $J/\psi \rightarrow \mu\mu$ mode. Note that, in spite of observed differences in the invariant lepton-pair mass and in the ΔE^* distributions for ee and $\mu\mu$, there is almost no difference in the shape of the p^* distributions. In Fig. 1, differences between data and simulation are seen on both edges of the signal peaks. They may arise from imperfections in describing the beam energy spread and the $Y(4S)$ line shape which influence B^0 and B^+ decays equally; the following data analysis has to account for the imperfections.

The mean values of the four $p^*(B)$ spectra are obtained from fits. The form of the fit functions is obtained from the MC spectra for “pure signal” and the sum of $B\bar{B}$ and $q\bar{q}$ backgrounds separately. For the signal, we find that a double-Gaussian function $S(p^*)$ with six parameters is adequate. Its parameters are: the number N of signal events (sum of classes 1 and 2), the mean \hat{p}^* and the rms width σ_{p^*} of $S(p^*)$, the fraction f of the subdominant Gaussian function, the peak-position difference Δ and the width ratio r_σ of the two Gaussian functions. The χ^2 fits of $S(p^*)$ to the “pure signal” contributions in the four spectra of Fig. 1 are of good quality. The fit-parameter values are similar in all four spectra; only the σ_{p^*} values are slightly larger in ee than in $\mu\mu$ decays. It has been checked that $S(p^*)$ with the same parameters as for “pure signal” also describes the p^* distributions of “signal with radiation” for both B^0 and B^+ decays.

The backgrounds for B^0 and B^+ are very different, requiring two different function types $U_0(p^*)$ and

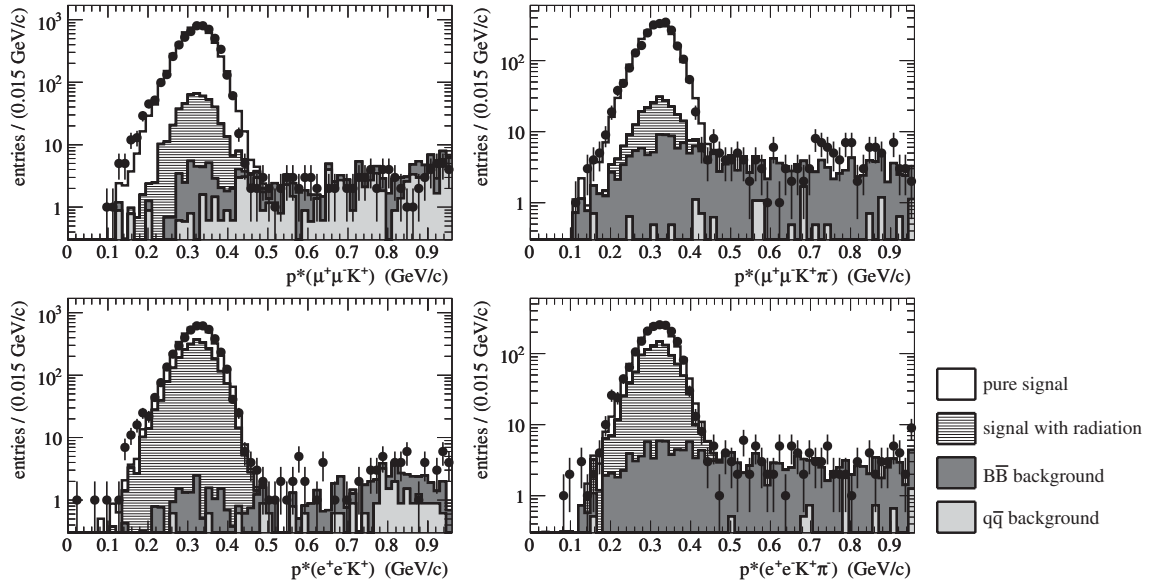


FIG. 1. The p^* distributions of the selected data (dots with error bars) and of the selected MC events (histograms stacked on top of each other). The left side is for B^+ , the right side for B^0 , the top for $J/\psi \rightarrow \mu\mu$, the bottom for $J/\psi \rightarrow ee$.

$U_+(p^*)$. We find that polynomials are adequate in both cases, linear for B^+ and of fifth degree for B^0 . The polynomials are determined by fits to the sum of the MC background histograms. Because of the complication with the mismatched signal MC events, we have to use fit functions $U_{0,+}(p^*) + S(p^*)$ for determining the background polynomials, where $S(p^*)$ is the best-fit signal function with free normalization.

In the fits of $S(p^*) + U_{0,+}(p^*)$ to the p^* distributions of real data, we choose binned maximum-likelihood fits between 0.12 and 0.95 GeV/c with bin widths of 0.015 GeV/c. The background polynomials are used with free normalizations r_{bg} but with shape parameters as given by the MC fits. In the signal function, all six parameters are left free since the signal shapes differ in data and MC because of the imperfect MC simulation. Since the \sqrt{s} spectrum dominates the shapes of the two p^* spectra, the parameters f , Δ , and r_σ are constrained to be equal for B^0 and B^+ .

Before fitting the real data, we apply the fit to p^* distributions of the MC simulation. We divide the sample of reconstructed MC events in five parts of equal size, each with the same integrated luminosity as the data. The 10 fit results, combining $J/\psi \rightarrow \mu\mu$ and ee , have a mean of $\Delta p^* = \hat{p}^*(B^0) - \hat{p}^*(B^+) = -4.7$ MeV/c with a rms of 0.4 MeV/c in good agreement with the MC input of -5.1 MeV/c.

Figure 2 shows the p^* distributions of the selected data events together with the best-fit functions. The fit results are given in Table I, and the derived Δp^* values are (-4.8 ± 1.1) MeV/c for the $J/\psi \rightarrow \mu\mu$ and (-6.4 ± 1.3) MeV/c for the $J/\psi \rightarrow ee$ mode. The two values are consistent, we therefore use the weighted mean

$$\Delta p^* = (-5.5 \pm 0.8) \text{ MeV/c}$$

for the final result. Before converting Δp^* into Δm_B , we present a number of cross-checks and the estimates of all contributions to the systematic uncertainty.

The Δp^* results from different run periods of the experiment are in agreement with each other and no charge dependence is observed. We find $\hat{p}^*(B^+) - \hat{p}^*(B^-) = -0.3 \pm 1.3$ (-1.0 ± 1.4) MeV/c for the $\mu\mu$ (ee) mode and $\hat{p}^*(B^0) - \hat{p}^*(\bar{B}^0) = 0.4 \pm 1.8$ (-1.2 ± 2.1) MeV/c for $\mu\mu$ (ee). Varying the ΔE^* requirements for the B candidates by factors of 1.4 up or down changes the central value of the Δp^* result by less than half a standard deviation. No sizable effect on the central value is seen when removing the requirement on the muon angle θ_H for the J/ψ candidates, on $m(K\pi)$, or on the event-shape parameter R_2 .

The contributions to the systematic uncertainty of Δp^* are summarized in Table II. The influence of the chosen parametrization for the signal fit-function is estimated by using modified parametrizations. First, we allow f , Δ , and r_σ to be different for B^0 and B^+ which results in $\Delta p^* = (-5.4 \pm 0.8)$ MeV/c. Second, we use one parameter less than in the nominal fit requiring $\sigma_{p^*}(B^0) = \sigma_{p^*}(B^+) \times \hat{p}^*(B^+)/\hat{p}^*(B^0)$ from Eq. (4) resulting in (-5.7 ± 0.8) MeV/c. We use the observed average variation of the three fit-method results in data and in the five MC validation subsamples as an estimate of the systematic uncertainty for the signal fit-function. Since the backgrounds are small, we also determine \hat{p}^* as algebraic means of the four p^* spectra between 0.12 and 0.45 GeV/c after subtracting the best-fit background functions. The results agree with those in Table I within

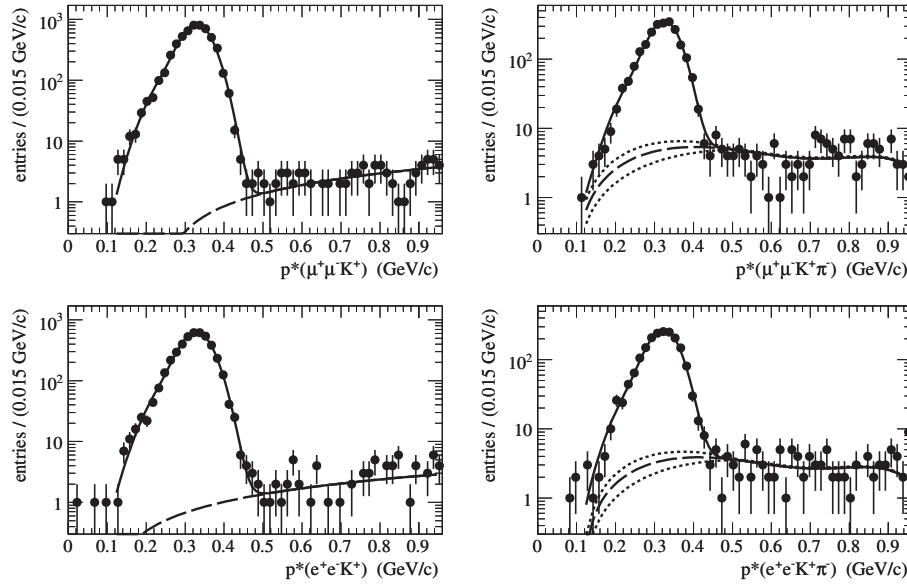


FIG. 2. The fitted p^* distributions in data, left side for B^+ , right side for B^0 , top for $J/\psi \rightarrow \mu\mu$, bottom for $J/\psi \rightarrow ee$. The dashed lines show the background polynomials; the dotted lines for B^0 show the changed backgrounds for the systematic-uncertainty estimate.

± 0.1 MeV/c except for $\hat{p}^*(B^0, ee)$ where it is 0.3 MeV/c lower.

The influence of the background in the $p^*(B^0)$ spectrum requires special care and was investigated by three methods. First, we compare the fit results for various ΔE^* cuts with r_{bg} free and $r_{bg} = 1$. Second, in order to control the influence of a slightly different background shape in the signal region, we fit the B^0 data using modified functions $\tilde{U}_0(p^*)$ with the arbitrary shapes of the two dotted lines in Fig. 2. Third, we select wrong-sign candidates in the channel $J/\psi K^+ \pi^+$ with all selection criteria as for the nominal B^0 candidates including those for $m(K\pi)$. The ratio Q of selected data and MC events is well approximated by the linear function $Q = 0.30 + 0.78 \times p^*/\text{GeV}$. The function $Q \times U_0(p^*)$ is then fitted to the selected B^0 data with r_{bg} floated. The second and third method give comparable shifts in $\hat{p}^*(B^0)$ and we take them as systematic uncertainty for the background-function; the

shift in the first method is 3 times smaller. Variations of the fit binning from the nominal 15 MeV/c width to 5, 10, and 20 MeV/c have a negligible influence. The transformation from laboratory-frame momenta to cms momenta has negligible influence, even by varying the applied boost by the five-fold of its rms in PEP-II. The detector influence on the Δm_B bias is estimated by using the MC results for the means $\hat{\delta}$ of $p^* - p_{\text{true}}^*$ as estimators for the uncertainties. The results are $\hat{\delta}(B^0) - \hat{\delta}(B^+) = (-0.14 \pm 0.13)$ MeV/c for the $\mu\mu$ and (0.25 ± 0.19) MeV/c for the ee mode. We conservatively use the sums of central value and rms of these results for the last-line entry in Table II.

Adding all systematic uncertainties in quadrature and taking the larger of the two estimates (ee) leads to

$$\Delta p^* = (-5.5 \pm 0.8 \pm 0.5) \text{ MeV/c}.$$

Inserted into Eq. (3) and using 319 MeV/c and 5279 MeV/c² for the mean values of B momentum and

TABLE I. Results for fitting the sum of signal and background functions to the four data p^* spectra in Fig. 2. The parameter N is the number of signal events and r_{bg} is the ratio of the observed to the simulated background level. The values for \hat{p}^* , σ_{p^*} , and Δ are in MeV/c.

	$B^0, \mu\mu$	$B^+, \mu\mu$	B^0, ee	B^+, ee
N	2280 ± 50	5580 ± 70	1820 ± 40	4350 ± 70
\hat{p}^*	316.8 ± 0.9	321.6 ± 0.6	314.7 ± 1.1	321.1 ± 0.7
σ_{p^*}	43.0 ± 0.8	44.4 ± 0.5	44.3 ± 0.9	45.4 ± 0.6
f		0.79 ± 0.04		0.78 ± 0.06
Δ		-51 ± 7		-48 ± 10
r_σ		1.46 ± 0.08		1.48 ± 0.08
r_{bg}	1.16 ± 0.10	1.01 ± 0.11	1.08 ± 0.11	1.93 ± 0.24

TABLE II. Summary of the systematic uncertainties for the measurement of Δp^* in MeV/ c .

	$\mu\mu$	ee
Signal Fit-Function	0.12	0.17
B^+ Background Fit-Function	0.01	0.03
B^0 Background Fit-Function	0.25	0.16
Histogram Binning	0.08	0.08
Detector Bias	0.27	0.44
Quadratic Sum	0.40	0.51

mass, we obtain

$$\Delta m_B = (+0.33 \pm 0.05 \pm 0.03) \text{ MeV}/c^2. \quad (5)$$

Contributions to the systematic uncertainty (in MeV/ c^2) come from Δp^* (± 0.031), the track-momentum uncertainty (± 0.011), and the mean- p^* -method bias (± 0.007). The contributions from the uncertainties on the $Y(4S)$ boost and the B -meson mass are negligible.

The Δm_B result in Eq. (5) is compatible with the present world average [2] of $(0.37 \pm 0.24) \text{ MeV}/c^2$ but the error is a factor of 4 smaller. The significance of Δm_B being positive exceeds the 5σ level. Inserting our Δm_B result into Eq. (1), we obtain $R_0 = 1.051 \pm 0.009$. The measured value of R is 1.037 ± 0.028 [2]. Given the agreement between these two results, we do not observe significant Coulomb or quark-structure contributions [4] to R .

We are grateful for the excellent luminosity and machine conditions provided by our PEP-II colleagues, and for the substantial dedicated effort from the computing organizations that support *BABAR*. The collaborating institutions wish to thank SLAC for its support and kind hospitality. This work is supported by DOE and NSF (USA), NSERC (Canada), CEA and CNRS-IN2P3 (France), BMBF and DFG (Germany), INFN (Italy), FOM (The Netherlands), NFR (Norway), MES (Russia), MEC (Spain), and STFC (United Kingdom). Individuals have received support from the Marie Curie EIF (European Union) and the A. P. Sloan Foundation.

-
- [1] W.M. Yao *et al.* (Particle Data Group), J. Phys. G **33**, 1 (2006).
 - [2] 2007 partial update for Ref. [1], <http://pdg.lbl.gov>.
 - [3] J.L. Goity and C.P. Jayalath, Phys. Lett. B **650**, 22 (2007) and references therein.
 - [4] S. Dubynskiy *et al.*, Phys. Rev. D **75**, 113001 (2007) and references therein.
 - [5] B. Aubert *et al.* (*BABAR* Collaboration), Nucl. Instrum. Methods Phys. Res., Sect. A **479**, 1 (2002).
 - [6] PEP-II Conceptual Design Report No. SLAC-418, 1993.
 - [7] The use of charge-conjugate states in this analysis is always implied.
 - [8] B. Aubert *et al.* (*BABAR* Collaboration), Phys. Rev. D **72**, 032005 (2005).
 - [9] S. Agostinelli *et al.* (GEANT4 Collaboration), Nucl. Instrum. Methods Phys. Res., Sect. A **506**, 250 (2003).
 - [10] E. Barberio and Z. Was, Comput. Phys. Commun. **79**, 291 (1994).
 - [11] G.C. Fox and S. Wolfram, Nucl. Phys. **B149**, 413 (1979).
 - [12] J. Schwiening *et al.* (*BABAR*-DIRC Collaboration), Nucl. Instrum. Methods Phys. Res., Sect. A **553**, 317 (2005).